*Proc. Natl. Acad. Sci. USA*
Vol. 92, pp. 3185–3189, April 1995
Biophysics

# Residue replacements of buried aspartyl and related residues in sensory rhodopsin I: D201N produces inverted phototaxis signals

**(seven-helix receptors/photosensory reception/bacteriorhodopsin/signal transduction)**

KARL D. OLSON, XUE-NONG ZHANG, AND JOHN L. SPUDICH

Department of Microbiology and Molecular Genetics, University of Texas Medical School, Health Science Center, Houston, TX 77030

*Communicated by Walther Stoeckenius, University of California, San Francisco, CA, December 5, 1994*

**ABSTRACT** **Residue replacements were made at five positions (Arg-73, Asp-76, Tyr-87, Asp-106, and Asp-201) in the *Halobacterium salinarium* phototaxis receptor sensory rhodopsin I (SR-I) by site-specific mutagenesis. The sites were chosen for their correspondence in position to residues of functional importance in the homologous light-driven proton pump bacteriorhodopsin found in the same organism. This work identifies a residue in SR-I shown to be of vital importance to its attractant signaling function: Asp-201. The effect of the substitution with the isosteric asparagine is to convert the normally attractant signal of orange light stimulation to a repellent signal. In contrast, similar neutral substitution of the four other ionizable residues near the photoactive site allows essentially normal attractant and repellent phototaxis signaling. Wild-type two-photon repellent signaling by the receptor is intact in the Asp-201 mutant, genetically separating the wild-type attractant and repellent signal generation processes. A possible explanation and implications of the inverted signaling are discussed. Results of neutral residue substitution for Asp-76 confirm our previous evidence that proton transfer reactions involving this residue are not important to phototaxis but that Asp-76 functions as the Schiff base proton acceptor in proton translocation by transducer-free SR-I.**

Sensory rhodopsin I (SR-I) is a 7-transmembrane helix phototaxis receptor structurally similar to the proton pump bacteriorhodopsin (BR) found in the same organism, *Halobacterium salinarium* (for review, see refs. 1–3). In both proteins, the chromophore retinal is attached in a protonated Schiff base linkage in the photoactive center of the molecule. In BR, photoisomerization of retinal drives proton release from the chromophore and its electrogenic translocation across the membrane (for review, see refs. 4 and 5). Five ionizable residues interacting with the chromophore in BR (Arg-82, Asp-85, Asp-96, Asp-115, and Asp-212) are involved in the transport mechanism. Most critically, Asp-85 is the primary acceptor of the Schiff base proton. Four of these residues are conserved in SR-I (Arg-73, Asp-76, Asp-106, and Asp-201), and SR-I, when separated from its normally tightly bound halobacterial transducer protein HtrI, carries out light-driven proton translocation with a mechanism similar to that of BR (6). In particular, Asp-76, corresponding to Asp-85 in BR, was suggested to function as the primary proton acceptor from the Schiff base. The pumping activity of SR-I depends on the deprotonation of a residue with $pK_a$ 7.2, which shifts the absorption maximum from 590 to 550 nm (6). This residue was suggested to be Asp-76, which is confirmed here by the observation that the Asp-76 to Asn substitution blocks the transition to the 550-nm form. The fifth residue in BR (Asp-96) is on the proton uptake path in the pumping cycle and is changed to a tyrosyl residue (Tyr-87) in SR-I.

The publication costs of this article were defrayed in part by page charge payment. This article must therefore be hereby marked "*advertisement*" in accordance with 18 U.S.C. §1734 solely to indicate this fact.

In wild-type membranes, SR-I is found in a complex with HtrI, which permits SR-I photoreactions to control the flagellar motors (7–10). HtrI prevents proton release from the membrane (9). Since Schiff base deprotonation is correlated with formation of the SR-I attractant signaling state (species $S_{373}$; SR-I photocycle species with absorption maximum at 373 nm) in the SR-I/HtrI complex, the protonatable residues important in BR may play a role in signaling by SR-I. We report here the site-specific mutagenesis of the corresponding five residues in SR-I and the effects on photochemical reactions and on phototaxis signaling.

## MATERIALS AND METHODS

**Plasmids and Strains.** Native and mutant forms of SR-I were expressed by transformation of *H. salinarium* strains Flx15Δ*sopI* ($SR\text{-}I^-HtrI^+$) (11) and Pho81W ($SR\text{-}I^-HtrI^-$). Mutagenesis was by cassette replacement in a synthetic *sopI* gene (11). Each of the plasmids denoted "tr" in this work encodes a protein that lacks the C-terminal 15 amino acids [termination at Ser-224 (9)], which enhances expression of SR-I and does not inhibit its function. Initially, the mutation was introduced into an *Escherichia coli* cloning vector. Plasmid DNA was isolated from a single *E. coli* transformant, and the mutated *sopI* gene was transferred to an expression vector capable of autonomous replication in *H. salinarium* (11). The mutation was confirmed in each case by sequencing through the mutation and ligation ends of the cassette. The mutation was reconfirmed by isolating the plasmid from one-half of the *H. salinarium* transformant colony or 1 ml of the culture and amplifying by PCR a fragment containing the mutation site. The fragment was subcloned into pBluescript KS+ (Stratagene) or pGEM5Zf(+) (Promega) and sequenced. The following primers were used for PCR, where restriction sites refer to those in the synthetic *sopI* gene: *Bam*HI site, 5′-TACCGGTCCCTCGATGG-3′; *Hin*dIII site, 5′-AGGTACGCGAACAAGC-3′; *Spe* I site, 5′-CGTGACCACGCCGATAC-3′; *Nsi* I site, 5′-GCTCAGCTCTCCGAATGCA-3′.

The following fragments were ligated to produce the indicated plasmids:

*pY87F.* Cloning vector: the 3075-bp *Spe I*/*Sph* I from pSO5, 457-bp *Sac* II/*Sph* I from pSO5, and 26-bp *Spe* I/*Sac* II cassette (encoding the replacement Tyr-87 to Phe). Expression vector: the 6.7-kbp *Hin*dIII/*Bam*HI from pMPK54, 2.4-kbp *Not* I/*Hin*dIII from pMPK39, 730-bp *Aat* II/*Not* I from pSO5 and 450-bp *Bam*HI/*Aat* II from pMPK39 (for a description of these fragments, see ref. 11).

*pR73Ntr.* Cloning vector: the 2832-bp *Not* I/*Aat* II fragment from pSO5, the 447-bp *Spe* I/*Not* I fragment from pTR1, the 217-bp *Aat* II/*Dde* I, and the 35-bp *Dde* I/*Spe* I cassette (encoding the replacement Arg-73 to Asn). Expression vector: fragments the same as those for pY87F except the 685-bp *Aat* II/*Not* I fragment from the cloning vector containing the Arg-73 to Asn mutation was used.

Abbreviations: BR, bacteriorhodopsin; SR-I, sensory rhodopsin I.

*pD106Ntr.* Cloning vector: the 2832-bp *Not* I/*Aat* II fragment from pTR-1, 300-bp *Aat* II/*Bgl* II fragment from pTR1, 404-bp *Not* I/*Bsp*HI fragment from pTR1, and 34-bp *Bgl* II/*Bsp*HI cassette containing the Asp-106 to Asn mutation. Expression vector: the ≈8-kbp *Bgl* II/*Sna*BI fragment from pTR2, ≈2-kbp *Bst*XI/*Sna*BI fragment from pTR2, and 240-bp *Bgl* II/*Bst*XI fragment from D106Ntr cloning vector.

*pD201Ntr.* Cloning vector: the 2832-bp *Not* I/*Aat* II fragment from pSO5, 580-bp *Aat* II/*Pst* I fragment from pSO5, 120-bp *Sty* I/*Not* I fragment from pTR1, and 46-bp *Pst* I/*Sty* I cassette (encoding the replacement Asp-201 to Asn). Expression vector: fragments the same as those for pY87F, except the 685-bp *Aat* II/*Not* I fragment from the *E. coli* cloning vector containing the Asp-201 to Asn mutation was used.

*pTR2, pD76Ntr, and pD76Atr.* Construction of these plasmids has been described (12).

*D201Ntr integrant.* The pD201Ntr plasmid was used to integrate the mutant *sopI* gene into the *bop* locus by a gene replace ment procedure (11).

A summary of the cassettes encoding each mutation is included in Table 1.

**Motion Analysis.** Motility responses to SR-I photoactivation were assayed by computer-assisted cell tracking and motion analysis as described (11). For action spectroscopy, the light intensity at various wavelengths selected by 10-nm bandwidth interference filters and neutral density filters (Corion, Holliston, MA) was measured at the position of the sample chamber with a radiometer (Kettering model 68; Scientific Instruments, West Palm Beach, FL). Fine adjustment of the light output from the tungsten/halogen lamp was made with a variable output transformer (Fisher Scientific). Pulse durations were controlled by a Uniblitz electronic shutter (Vincent Associates, Rochester, NY). Phototaxis stimuli were delivered through an epiilluminator from a Nikon 100-W Hg/Xe lamp in Table 1 and from a 150-W tungsten/halogen lamp beam conducted to the epiilluminator via a fiber optic at the intensities indicated in Figs. 3 and 4.

**Flash Photolysis.** Flash-induced absorption changes were recorded with a laboratory-constructed cross-beam flash spectrometer. Ten to 20 transients were averaged for each measurement. The actinic flash was delivered at 0.1 Hz with a pulsed Nd:YAG (yttrium/aluminum garnet) laser (pulse width, 6 ns; 40 mJ) at 532 nm (Surelite I; Continuum, Santa Clara, CA). Rate constants and amplitudes were obtained by fitting the data to single or multiple exponentials by using the curve-fitting algorithm from SigmaPlot (Jandel, Corte Madera, CA).

**Growth Conditions.** All strains of *H. salinarium* were grown as described (11) except cultures used for motion analysis were grown in 200 ml of complex medium.

**Membrane Preparations.** The membrane fraction was isolated from sonicated early stationary phase cells as described (9). The final suspension (in 4 M NaCl/25 mM Tris·HCl, pH 6.8) of membranes was 8–10 mg of protein per ml as determined by the Lowry assay (Sigma). Membranes were pelleted for 20 min at 75,000 rpm in a Beckman TL-100 tabletop ultracentrifuge.

Table 1. Summary of cassettes encoding each mutation

| Mutant | Mutation | Cassette | Phototaxis* | |
|---|---|---|---|---|
| | | | Attractant | Repellent |
| SRtr | † | † | 1.00 | 1.00 |
| Y87F | TAC → TTC | *Spe* I/*Sac* II | 0.91 | 0.77 |
| D76Atr | GAC → GCC | *Dde* I/*Spe* I | 1.09 | 0.86 |
| D76Ntr | GAC → AAT | *Dde* I/*Spe* I | 0.43 | 1.25 |
| R73Ntr | AGG → AAC | *Dde* I/*Spe* I | 1.17 | 0.40 |
| D106Ntr | GAC → AAC | *Bgl* II/*Bsp*HI | 0.80 | 0.35 |
| D201Ntr | GAC → AAC | *Pst* I/*Sty* I | Inverted | 0.25 |

*The increase in reversal frequency above the prestimulus value integrated for 1 sec after initiation of the peak. Reversal responses to step-down attractant (600 nm) and step-up repellent (400 nm) stimuli were normalized to the responses of pTR2/Flx15Δ*sopI*, which were 0.37 and 0.47 $sec^{-1}$, respectively.

†Construction described in ref. 9.

## RESULTS

**Photochemical Reactivity.** The time course of absorbance changes for each mutant and native SR-I in its C-terminally truncated form (SRtr) expressed in the presence of HtrI was monitored at 590 nm (lower transient) and 400 nm (upper transient) after a flash (Fig. 1 *Left*). Half-times from exponential decay fits are shown for each trace. In Flx15Δ*sopI*/SRtr vesicles (in which SR-I is expressed at severalfold higher than wild-type levels), we observed three components in the recovery of 590-nm absorbance after a flash at pH 6.8: (*i*) a fast component ($t_{1/2}$ = 16 msec), (*ii*) an approximately wild-type component ($t_{1/2}$ = 500 msec), and (*iii*) a slow component ($t_{1/2}$ = 6.2 sec). The $t_{1/2}$ values displayed in Fig. 1 do not include the 16-msec component. Comparison of transients in transducer-free (8, 12) and transducer-containing membranes (9, 11) indicates the fast and slow components derive from transducer-free SR-I, and the wild-type component derives from transducer-complexed SR-I. The transducer-complexed component is pH insensitive, unlike the transducer-free slow component (slow at pH 6.8) (8). The 16-msec component was not observed at 400 nm. Its absorption difference spectrum (data not shown) indicates formation and decay of a blue-shifted intermediate(s) ($\lambda_{max}$, 520–560 nm).

Among the mutants, only D76Ntr and D76Atr exhibited significant transducer-free components (corresponding to *i* and *iii* above). In D76Ntr the transducer-complexed $S_{373}$ decay, as assessed by its pH independence (data not shown), was approximately equal in rate to the transducer-free slow component at pH 6.8. Therefore, only a single $t_{1/2}$ is shown. The D76Atr slow components (4.6 and 8.4 sec) were accelerated at lower pH and therefore are interpreted as transducer-free values. The transducer-complexed (i.e., pH independent) half-times, 0.7 and 0.8 sec in this particular curve fit, varied between 0.7 and 3 sec in other measurements with an average of 1.9 sec. The other mutants exhibited essentially first-order decays, which were approximately wild type for Y87F, slower for R73Ntr and D201Ntr, and slightly faster than wild type in the case of D106Ntr.

As shown in Fig. 1, we obtained variable amounts of photoactivity; the highest amount was produced in the SRtr case, with slightly less in D76Ntr and D76Atr, and much less (≈10%) produced in the cases of D106Ntr, D201Ntr, and R73Ntr. In these three cases, greatly reduced pigment content was evident in absorption measurements (data not shown). Little or no fast component was observed in R76Ntr, Y87F, D106Ntr, and D201Ntr-containing vesicles, consistent with relatively low levels of receptor in these cases—i.e., all of the receptor is complexed with HtrI. Supporting this conclusion, their photocycle rates were similar at pH 5.8 to those at pH 6.8 (Fig. 1).

**Phototaxis Signaling.** SR-I mediates both attractant and repellent responses depending on wavelength (13). When the mutant SR-I or SRtr proteins were produced in Flx15Δ*sopI*, which contains the SR-I transducer HtrI, the cells exhibited approximately normal color-sensitive phototaxis responses (Table 1) with the exception of D201Ntr (see below). Smaller responses (<50%) occurred in a few cases and may be due to a reduction of signaling efficiency or lower receptor content. Response peaks were delayed for 1–2 sec after a step-down in attractant light in cells containing D76N, D76A, and R73N (data not shown). We have previously concluded that the reduction of $S_{373}$ concentration produces the reversal-inducing signal in response to a step-down in attractant light on the basis

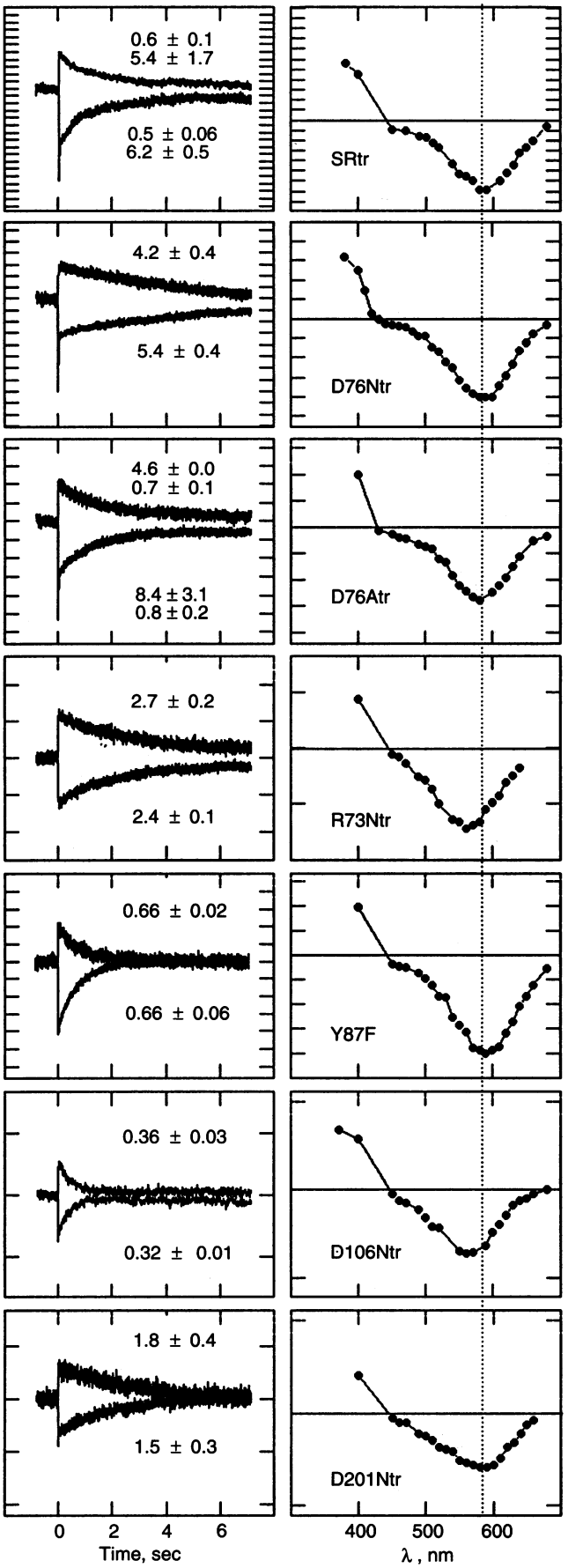


FIG. 1. Flash-induced absorption difference transients and spectra of SRtr and mutant receptors in Flx15Δ*sopI* membranes. Each tick mark along the ordinate represents $9 \times 10^{-4}$ absorption units. Membrane envelope vesicles were suspended at 1.25 mg of protein per ml (SRtr, D76Atr, and D76Ntr) or 2.5 mg of protein per ml (Y87F, D106Ntr, and D201Ntr). Final absorption changes are expressed per 1.25 mg of protein per ml in all cases. (*Left*) Time course of absorbance changes monitored at 590 nm (lower transient) and 400 nm (upper transient) after a flash at time 0. The rate constant for each return is shown next to its transient (values are in sec ± SEM; $n = 2$ or 3). (*Right*) Absorption changes 100 ms after the flash. Each value is the average from two or three transients. Vertical dotted line indicates 590 nm. C-terminally truncated proteins are designated tr.

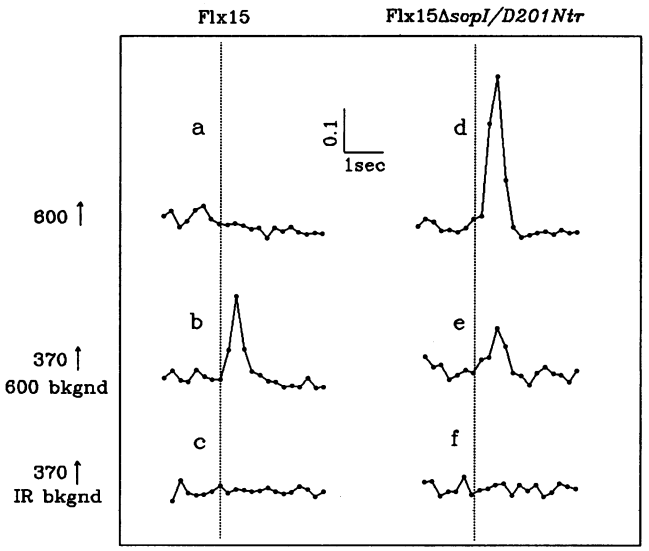


FIG. 2. Population reversal frequencies vs. time. Dark-field microscopy video data were processed at 5 frames per sec and reversal frequencies were measured as the number of reversals detected within the 200-msec frame interval per number of paths present in that interval. Reversal frequency transients for Flx15 cells (*Left*) and Flx15Δ*sopI/D201Ntr* cells (*Right*) are shown for stimuli delivered at the time indicated by the vertical dotted line. (*Top*) A 4-sec step-up in orange light (600 ± 20 nm), $3.8 \times 10^3$ erg·cm$^{-2}$·sec$^{-1}$. (*Middle*) A 200-msec step-up in violet light (370 ± 5 nm) in a 600-nm background. (*Bottom*) A 200-msec step-up in violet light (370 ± 5 nm) in a nonactinic infrared background.

of retinal analogue receptors with altered $S_{373}$ decay kinetics (1). The delayed attractant responses may therefore reflect the lower $S_{373}$ decay rates in D76N, D76A, and R73N compared to native SR-I. Responses with wild-type kinetics were observed in cells containing the Y87F receptor, consistent with the approximately wild-type lifetime of $S_{373}$.

**Inverted Signaling by D201N.** The wild-type (Flx15) response to orange (600 nm) light is suppression of reversals, since orange light is normally an attractant (Fig. 2, trace a). In the case of Flx15Δ*sopI/D201Ntr* (i.e, D201Ntr integrated into the chromosome of a SR-I$^-$SR-II$^+$ strain), however, a large increase in population reversals was observed—i.e., a repellent response (trace d). This is the opposite response of any of the other mutants examined (Table 1). A step-down in orange light does not induce and may suppress reversals in Flx15Δ*sopI/D201Ntr*, also the opposite of wild type (data not shown).

The SR-I$^-$SR-II$^+$ strain Flx15Δ*sopI* exhibits no response to low or high orange light intensities. At high light intensities, a small repellent response occurs to a step-up in 500-nm light (Fig. 3 *Upper*), as expected from the presence of SR-II ($\lambda_{max}$ = 480 nm). The repellent response of Flx15Δ*sopI/D201Ntr* to orange light (Fig. 2), however, is not attributable to SR-II. This is evident from the wavelength and intensity dependence (Fig. 3 *Lower*), since 580 nm is more effective than 500 nm (Fig. 3), and the wavelength dependence of the inverted response

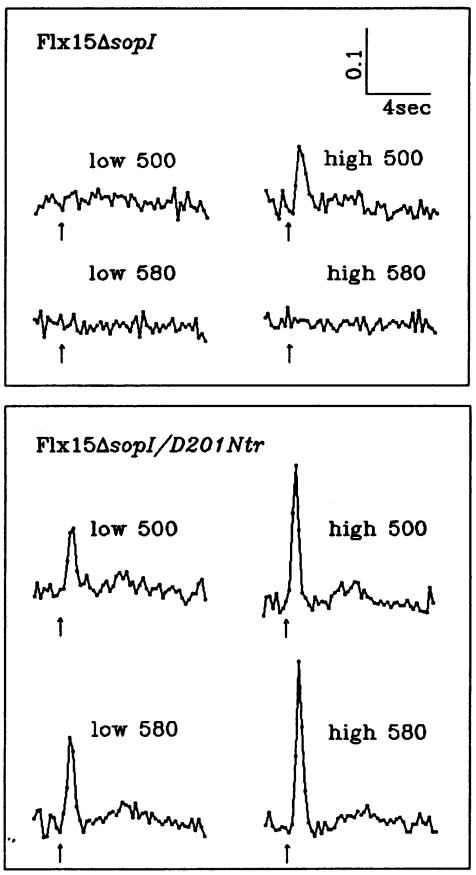


FIG. 3. Motility responses to 500- and 580-nm photostimuli. At the arrow, light (500 ± 20 nm or 580 ± 20 nm) was delivered for 4 sec. (*Upper*) Reversal responses of Flx15Δ*sopI* (SR-I$^-$SR-II$^+$) cells at either low (*Left*) or high (*Right*) light intensity stimuli of $1.6 \times 10^2$ and $3.8 \times 10^3$ erg·cm$^{-2}$·sec$^{-1}$, respectively. (*Lower*) Reversal responses of Flx15Δ*sopI/D201Ntr* transformants to the same stimuli.

roughly matches the absorption depletion in the flash-induced difference spectrum due to the D201N pigment (Fig. 4).

In the case of Flx15Δ*sopI/D201Ntr*, we observed reversal induction by 370-nm blue light, which depended on an orange-light (600 nm) background as we also observe for Flx15 (Fig. 2, traces b, c, e, and f). This pattern of responses is attributable to the $S_{373}$ repellent receptor activity, since an orange light is needed to generate a photostationary state containing $S_{373}$ (13). Hence, the $S_{373}$ repellent response is not inverted in the mutant.

**pH Effects on the Receptors.** SRtr and the mutated genes were also expressed in Pho81W, a strain lacking HtrI (14). The wavelength of maximum flash-induced absorbance depletion was determined at various pH values (Fig. 5). In Pho81W/SRtr vesicles, as reported previously, the depletion shifts from ≈590 nm at pH 7.0 to ≈550 nm at pH 8.0 with an apparent $pK_a$ of 7.2 (see ref. 6 and Fig. 5). No shift was observed in the case of Pho81W/D76Ntr or Pho81W/D76Atr (tested to pH 8.7). We also varied the pH of a Flx15Δ*sopI/D76Ntr* vesicle suspension and observed no change in the flash-induced depletion spectrum between pH 6.8 and pH 8.9.

As occurs with D106Ntr expressed in the presence of HtrI (in Flx15Δ*sopI*) (Fig. 1), vesicles of Pho81W/D106Ntr showed a maximum flash-induced depletion at ≈560 nm. Upon shifting the pH of the suspension to pH 8.9, the depletion shifted to 540 nm, with a $pK_a$ of ≈8. Hence, the depletion maxima and the $pK_a$ of the spectral transition are affected by this mutation.

## DISCUSSION

The results above identify the first residue in SR-I shown to be of vital importance to its attractant signaling function: Asp-

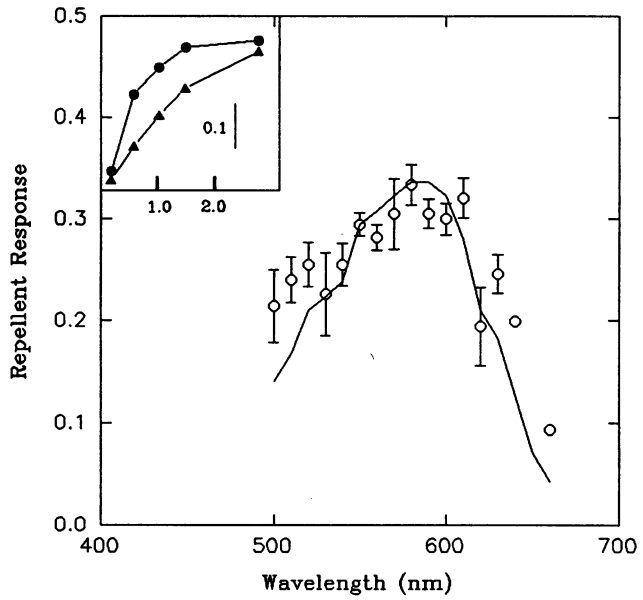


FIG. 4. Wavelength dependence for the repellent response of Flx15Δ*sopI/D201Ntr* cells. Points were calculated as the average of three to five independent measurements and error bars ± SEM. The flash-induced absorption depletion of the D201Ntr receptor in vesicles at pH 6.8 was taken from Fig. 1, inverted, and overlaid. Equivalent energy of light at each wavelength was delivered to the cells ($1.6 \times 10^2$ erg·cm$^{-2}$·sec$^{-1}$). (*Inset*) Reversal response in sec$^{-1}$(ordinate) is plotted as a function of stimulus intensity (abscissa; $\times 10^3$ erg·cm$^{-2}$·sec$^{-1}$) at 580 nm (solid circles) and 500 nm (solid triangles).

201. The effect of substitution with the isosteric asparagine is to convert the normally attractant signal from orange light stimulation to a repellent signal. $S_{373}$-mediated repellent signaling by SR-I is intact in D201N. The D201N results, therefore, genetically separate the attractant and repellent signal generation processes, which were previously concluded to be distinct based on photophysiological measurements (13).

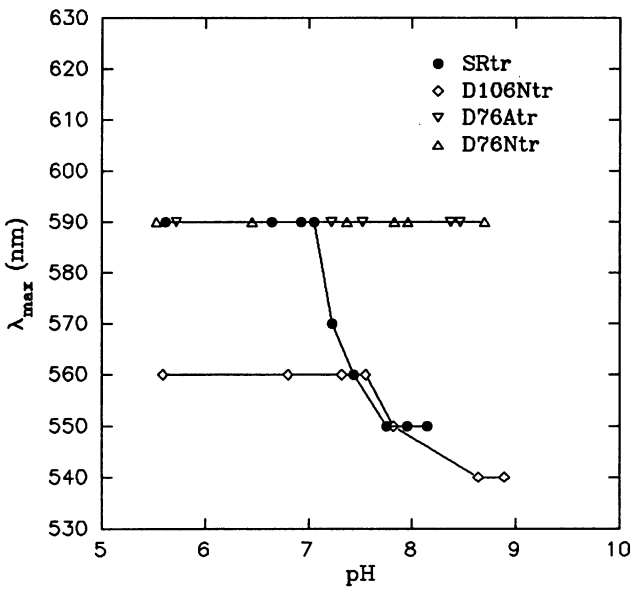


FIG. 5. $\lambda_{max}$ of SRtr and various mutants expressed in the absence of HtrI vs. pH. $\lambda_{max}$ values were determined from the flash-induced absorbance changes measured at 10-nm intervals. Each sample was at 5 mg of protein per ml in 4 M NaCl (final vol, 2 ml). Microliter volumes of HCl or NaOH were added to the preparation with stirring and the pH was measured.

Inverted responses to orange light have been reported previously under conditions of repetitive stimulation (15, 16). Although the mechanism is not known, it appears that orange light-adapted cells, if not given sufficient time to de-adapt after orange light is removed, exhibit inverted responses (i.e., reversals) to an orange light pulse delivered up to 10 sec into the dark period. Therefore, a possible explanation for the D201N inversion is that cells containing the mutated receptor are in an orange light-adapted state in the dark. This state would imply the D201N is locked in a constitutively active attractant signaling mode. Adaptation to the constant attractant signal would occur just as it does in continuous orange light. The inverted responses by repetitive stimulation and the D201N inversion may therefore have the same basis: an inappropriately attractant-adapted complex in the dark.

Asp-201 corresponds to Asp-212 in BR, which is near the Schiff base nitrogen. This raises the possibility that Asp-201 functions as the Schiff base proton acceptor during attractant activation, and for this reason D201N exhibits the conformation of the attractant signaling state. In this regard, it is interesting that genetic neutralization of the Schiff base proton acceptor in human rod rhodopsin results in constitutive signaling (17). However, if this is so in the case of SR-I there must be alternative proton acceptors since photoreaction of D201N produces an $S_{373}$-like intermediate. When the proton acceptor in BR, Asp-85, is replaced with a neutral residue the proton is released to the opposite side of the membrane (18). Altered release of the Schiff base proton in D201N may be involved in its inverted signaling.

None of the residues, Arg-73, Asp-76, Tyr-87, or Asp-106, is individually essential for the generation of an $S_{373}$-like intermediate or attractant or repellent phototaxis signals by SR-I. Absorption maxima of R73Ntr and D106Ntr are shifted 20–30 nm, as deduced from the flash-induced difference spectra. This result argues that Arg-73 and Asp-106 are structurally important residues but argues against their direct involvement in signaling.

**Asp-76 and the Pumping Form of SR-I.** Under certain conditions, SR-I can function as an electrogenic proton pump (6). A key residue involved in mediating proton pumping in BR is the Schiff base proton acceptor, Asp-85, which together with Asp-212 and Arg-82 forms a counterion for the protonated Schiff base (19–23). When Asp-85 is protonated by lowering the pH or substituted with a neutral residue, the absorption maximum of BR shifts from 568 to ≈590 nm and the pumping activity is eliminated (24). HtrI-free SR-I exhibits a similar spectral transition from a 550-nm pumping form to a non-pumping 590-nm form (6) and Asp-76 is neutral in the 590-nm form (12). The data presented here show that the D76N and D76A mutants of SR-I do not undergo this spectral transition (tested between pH 5.5 and 8.7). Our interpretation is that Asp-76 deprotonates in the 590- to 550-nm transition of HtrI-free SR-I. Ionized Asp-76 can then accept a proton from the Schiff base and release it to the exterior in a manner analogous to Asp-85 in BR (4, 5).

We thank Elena Spudich for her help in constructing the plasmids; Walther Stoeckenius and Roberto Bogomolni for stimulating discussions; and Jutta Seufert, Joachim Scholz-Starke, Ewa Lukomska, and Marcella Cervantes for helpful assistance. This research was supported by Grant GM27750 from the National Institutes of Health to J.L.S. and Postdoctoral Fellowship PF-3806 from the American Cancer Society to K.D.O.

1. Spudich, J. L. & Bogomolni, R. A. (1992) *J. Bioenerg. Biomembr.* **24,** 193–200.
2. Oesterhelt, D. & Marwan, W. (1993) in *The Biochemistry of Archaea (Archaebacteria)*, ed. Kates, M. (Elsevier, Amsterdam), pp. 173–187.
3. Spudich, J. L. (1994) *Cell* **79,** 747–750.
4. Lanyi, J. K. (1993) *Biochim. Biophys. Acta* **1183,** 241–261.
5. Krebs, M. P. & Khorana, H. G. (1993) *J. Bacteriol.* **175,** 1555–1560.
6. Bogomolni, R. A., Stoeckenius, W., Szundi, I., Perozo, E., Olson, K. D. & Spudich, J. L. (1994) *Proc. Natl. Acad. Sci. USA* **91,** 10188–10192.
7. Yao, V. & Spudich, J. L. (1992) *Proc. Natl. Acad. Sci. USA* **89,** 11915–11919.
8. Spudich, E. N. & Spudich, J. L. (1993) *J. Biol. Chem.* **268,** 16095–16097.
9. Olson, K. D. & Spudich, J. L. (1993) *Biophys. J.* **65,** 2578–2586.
10. Krah, M., Marwan, W., Vermeglio, A. & Oesterhelt, D. (1994) *EMBO J.* **13,** 2150–2155.
11. Krebs, M. P., Spudich, E. N., Khorana, H. G. & Spudich, J. L. (1993) *Proc. Natl. Acad. Sci. USA* **90,** 3486–3490.
12. Rath, P., Olson, K. D., Spudich, J. L. & Rothschild, K. J. (1994) *Biochemistry* **33,** 5600–5606.
13. Spudich, J. L. & Bogomolni, R. A. (1984) *Nature (London)* **312,** 509–513.
14. Yao, V. J., Spudich, E. N. & Spudich, J. L. (1994) *J. Bacteriol.* **176,** 6931–6935.
15. Hildebrand, E. & Schimz, A. (1987) *J. Bacteriol.* **169,** 254–259.
16. McCain, D. A., Amici, L. A. & Spudich, J. L. (1987) *J. Bacteriol.* **169,** 4750–4758.
17. Robinson, P. R., Cohen, G. B., Zhukovsky, E. A. & Oprian, D. D. (1992) *Neuron* **9,** 719–725.
18. Tittor, J., Schweiger, U., Oesterhelt, D. & Bamberg, E. (1994) *Biophys. J.* **67,** 1682–1690.
19. Braiman, M. S., Mogi, T., Marti, T., Stern, L. J., Khorana, H. G. & Rothschild, K. J. (1988) *Biochemistry* **27,** 8516–8520.
20. Holz, M., Drachev, L. A., Mogi, T., Otto, H., Haulen, A. D., Heyn, M. P., Skulachev, V. P. & Khorana, H. G. (1989) *Proc. Natl. Acad. Sci. USA* **86,** 2167–2171.
21. Otto, H., Marti, T., Holz, M., Mogi, T., Lindau, M., Khorana, H. G. & Heyn, M. P. (1989) *Proc. Natl. Acad. Sci. USA* **86,** 9228–9232.
22. Gerwert, K., Hees, B., Soppa, J. & Oesterhelt, D. (1989) *Proc. Natl. Acad. Sci. USA* **86,** 4943–4947.
23. Dér, A., Száraz, S., Tóth-Boconádi, R., Tokaji, Z., Keszthelyi, L. & Stoeckenius, W. (1991) *Proc. Natl. Acad. Sci. USA* **88,** 4751–4755.
24. Subramanium, S., Marti, T. & Khorana, H. G. (1990) *Proc. Natl. Acad. Sci. USA* **87,** 1013–1017.